SCIENCE CHINA
Earth Sciences

•RESEARCH PAPER•

May 2020 Vol.63 No.5: 713–725
https://doi.org/10.1007/s11430-019-9533-8

Groundwater net discharge rates estimated from lake level change in Badain Jaran Desert, Northwest China

Xingfan WANG[1,3], Hui ZHAO[1,2*], Yongwei SHENG[4], Jianwei GENG[1,3], Keqi WANG[1,3] & Hongyu YANG[1,3]

[1] *Key Laboratory of Desert and Desertification, Northwest Institute of Eco-Enviroment and Resources, Chinese Academy of Sciences, Lanzhou 730000, China;*
[2] *CAS Center for Excellence in Tibetan Plateau Earth Sciences, Chinese Academy of Sciences, Beijing 100101, China;*
[3] *University of Chinese Academy of Sciences, Beijing 100049, China;*
[4] *Department of Geography, University of California, Los Angeles, CA 90095, USA*

Received February 25, 2019; revised September 20, 2019; accepted October 22, 2019; published online December 31, 2019

Abstract Over a hundred sizable lakes, some even larger than ~1 km^2, are distributed across the lowlands between megadunes in the southeastern Badain Jaran Desert (BJD), northwest China. With rather limited precipitation and hardly any surface runoff, these lakes are fed mainly by groundwater. However, the source of the groundwater and the groundwater discharge rates to these lakes are poorly understood. Water level and temperature of four representative lakes in the southeastern BJD were monitored continuously between 2013 and 2017. Water surface evaporation and rainfall in this area were also measured. Combining these acquired data, groundwater discharge rates were estimated using water balance models. The results show that the four lakes have similar recharge and discharge patterns, but at different average net groundwater discharge rates ranging from 1.79 to 3.09 mm d^{-1}. The lake level variation mainly depends on groundwater discharge and lake surface evaporation. We found that diurnal lake level variation may be controlled by earth tide and atmospheric pressure change, and is five times greater than the evaporation. The desert precipitation and deep confined groundwater with high temperature were found also recharging the desert lakes. An Empirical Mode Decomposition (EMD) method was used to identify the lake level trend. All lake levels increased over the last four years, except one decreased in 2015 and 2016. The lake levels' increasing trend is synchronously similar with the precipitation in north China. This study analyzes annual and seasonal lake level variations, and also finds the diurnal water cycle between the groundwater and lake water for the first time.

Keywords Groundwater discharge, Lake level, Water balance, Badain Jaran Desert

Citation: Wang X, Zhao H, Sheng Y, Geng J, Wang K, Yang H. 2020. Groundwater net discharge rates estimated from lake level change in Badain Jaran Desert, Northwest China. Science China Earth Sciences, 63: 713–725, https://doi.org/10.1007/s11430-019-9533-8

1. Introduction

The Badain Jaran Desert (BJD) is on the Alxa Plateau in northwestern China, covering an area of 4.92×10^4 km^2 (Zhu et al., 1980) between 99°54′–104°34′E and 39°20′–41°19′N. It is surrounded by the Yabrai mountain to the southeast, the Beida to the southwest, the alluvial fan of Heihe River to the northwest, and the Guaizihu wetland to the north (Figure 1a). Located at the far end of the Asia summer monsoon, the desert is controlled by an extreme continental climate (Gao et al., 2006). Dominated by cold and dry continental air masses originating from mid-Siberia and Mongolia, the winter monthly mean temperature is about 4°C with little precipitation. Affected by the East Asian monsoon, the summer monthly mean temperature is ~24°C with limited precipitation. Annual mean precipitation is concentrated in July and

* Correspondence author (email: hzhao@lzb.ac.cn)

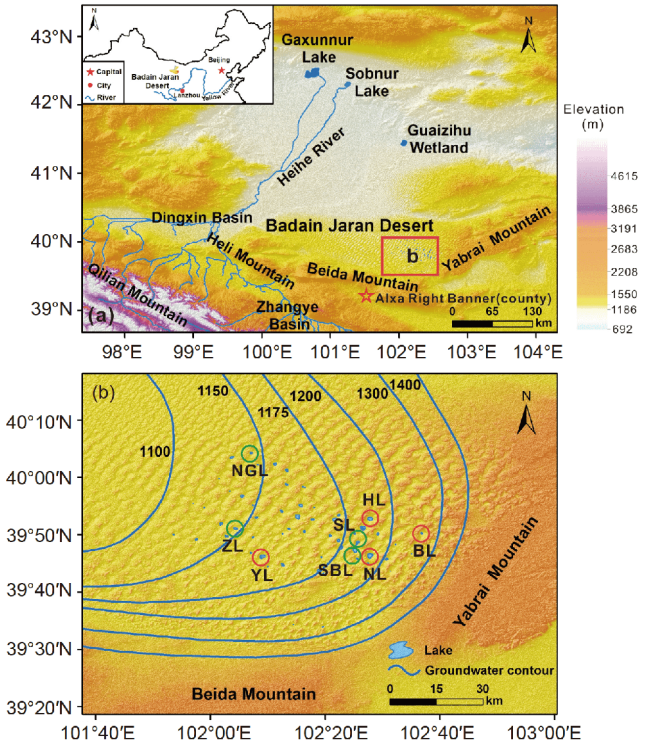

Figure 1 Location and topographic map of Badain Jaran Desert. (a) Distribution of studied lakes and groundwater level countours based on lake level altitude estimated using Google Earth and Zhang et al. (2015); (b) lakes in present study are shown by open red circles, and previously reported lakes by open green circles. SBL: Sumubarunjilin Lake (Dong et al., 2016); SL: Sumujilin Lake (Wang et al., 2014); ZL: Zhaoergetu Lake (Dong et al., 2016); NGL: Naogunnuoer Lake (Dong et al., 2016).

August, ranging from 37 mm in the northwestern desert to 118 mm in the southeast (Yang et al., 2003). Comparing to the low precipitation, potential evaporation is extremely strong, from 2600 to 4000 mm (Chen et al., 2004a; Yang et al., 2011; Gates et al., 2008b). The desert is well known for its unique landscape of megadunes coexisting with lakes. About 100 lakes of various sizes (from hundreds square meters to ~1 km^2) and salinities (0.01–345.0 g L^{-1}) are distributed across the lowland of megadunes in the southeastern part of the desert (Zhu et al., 1980; Dong et al., 2013).

The water sources of the large group of lakes in such an arid desert have been a hot topic and have been widely investigated in recent decades (Dong et al., 2013). Because there is hardly any surface runoff into these lakes and the limited precipitation over the lakes are insufficient to balance the high evaporation, the lakes are mainly supplied by desert groundwater. However, the source of the groundwater is still under debate. Four possible groundwater sources have been posited: (1) phreatic water is supplied by local precipitation according to the strong water penetrability of sand and findings of infiltration-excess runoff traces (Ma et al., 2017; Zhao et al., 2017; Yang et al., 2010; Yang and Williams, 2003; Hou et al., 2016); (2) rainfall in the mountain area surrounding the desert is also likely one of the main sources of the groundwater (Ma et al., 2007; Huang and Pang, 2007; Gates et al., 2008a; Shao et al., 2012; Wu et al., 2017); (3) the $^{87}Sr/^{86}Sr$ ratio of the groundwater and tufa in the desert lakes indicates that the groundwater may be recharged by deep groundwater from fault zones of the Qilian Mountains or Qinghai-Tibetan Plateau (Chen et al., 2003, 2004a, 2004b; Zhao and Chen, 2006); (4) limnic relics in the desert indicate that the groundwater and lakes have residual paleo-water originating from paleo-lakes appearing during the humid period of the late Pleistocene (Yan et al., 2001; Ma and Edmunds, 2006; Huang and Pang, 2007; Zhang et al., 2015). Although progress has been made in previous water origin investigations, the groundwater source remains controversial since most inferences were made based on limited hydrogeochemistry and isotopic data and there is a lack of direct hydrologic observations such as lake level, precipitation, and evaporation in the desert.

Groundwater discharge rates and lake level changes are crucial for us to understand the source and balance of lake water in the BJD. Based on the distance between the lakeshore and poplars planted on the lake bank by local herdsmen, Yang and Williams (2003) first reported desert lake level and area changes, indicating that the lake surface shrank ~10% from 1983 to 1999. In recent years, remote sensing data including Landsat imagery have been used to analyze lake area seasonal and inter-annual change (Zhu et al., 2011; Zhang et al., 2012, 2013). In addition, ICEsat data have been used to estimate annual lake level variation (Jiao et al., 2015). The results show that both lake area and level had an overall declining trend in recent decades, but with strong seasonal variabilities. However, owing to limitations of the remote sensing data, the numbers of lake area and level observations were somewhat limited and discontinuous, so lake water variation could only be roughly estimated.

In recent years, short-term lake level observation data in BJD have been presented (Wu et al., 2014; Gong et al., 2016; Dong et al., 2016; Luo et al., 2016). Luo et al. (2016) showed only two-day observation data, and the temporal groundwater discharge rate was calculated using an isotope mass balance model (Luo et al., 2016, 2017). Dong et al. (2016) obtained one-year data of one lake, and calculated groundwater discharge using a water balance method. However, inter-annual lake level change and recharge of different lakes remains untouched. Hence, multi-lake groundwater discharge rates and long-duration lake level variation are essential for us to understand groundwater and lake water interaction.

To ascertain groundwater discharge rate and its relationship with lake level variation, between 2013 and 2017 we continuously collected water level and temperature measurements in four lakes (Figure 1b) over 10 km apart with

different size and salinity. Precipitation and lake surface evaporation were also monitored during the same period. Because there is no surface runoff to the studied lakes, the groundwater net discharge was calculated based on those measured data using a lake water balance method. In addition, the potential groundwater recharge sources are also discussed.

2. Materials and methods

2.1 Site description

Four lakes were selected for water level and temperature measurement, i.e., Boerzongtu Lake (BL), Nuoertu Lake (NL), Huhejilin Lake (HL) and Yihejigede Lake (YL) (Figure 1b). BL is a shallow brackish-water lake in the eastern BJD, close to the Yabrai Mountain, while HL is a deep saline lake 13 km away in the northwest. As the largest salt lake in the desert, NL is in the lowland of the highest megadune, ~13 km southwest of BL. YL is a shallow saline lake ~60 km west of the Yabrai Mountain and ~40 km north of the Beida Mountain (Figure 1b). Along the shores of BL, HL and NL, there are seepage zones with groundwater flow into these lakes. Lake elevation decreases from ~1200 m in the southeast to ~1150 m in the northwest, producing a hydraulic gradient (Figure 1b). Lake surface area was mapped using Landsat-8 remote sensing images, and is shown in Table 1 together with other lake characteristics.

2.2 Stratigraphy and hydrogeology characteristics

In the BJD hinterland, Quaternary incompact sediments constitute the main body of the aquifers underlying modern lakes, which was revealed by a drill core in the central desert (Wang et al., 2015). Quaternary deposits around the modern lakes can be divided into three main aquifers from top to bottom (Zhang et al., 2017). The first one is an unconfined aquifer with a hydraulic conductivity of 3–20 m d^{-1} and porosity of 0.35–0.45 (Wang et al., 2014), constituted by the Holocene aeolian sand and late Pleistocene lacustrine fine-sand with a thickness of 10 m in the modern lowlands between megadunes. This aquifer directly linked with the precipitation infiltration and evaporation processes (Zhang, 2015). The second aquifer is the confining bed of the underlying confined water with a hydraulic conductivity of 0.05–0.25 m d^{-1}. This aquifer is constituted by the late Pleistocene lacustrine sandy loam and sub clay with the thickness less than 10 m and deposit age about 100 ka (Wang et al., 2015). The bottom aquifer is a confined aquifer with a hydraulic conductivity of 0.5–5.0 m d^{-1}, constituted by the middle Pleistocene sand layer older than 300 ka (Wang et al., 2015). These aquifers imply that the groundwater should mainly exit in the bottom middle Pleistocene sand layer, groundwater passes through the crevices of the compaction lacustrine layer to supply the modern lakes. The widely existed ascending springs besides or in the modern lakes also support that implication.

2.3 Data collection

Water level and temperature were monitored hourly from Jun 24, 2013 to Feb 15, 2017 using self-recording water level dataloggers (Solinst® Levelogger) at all four lakes (BL, HL, NL and YL). Only two-year data (Jun 24, 2013 to Jun 29, 2015) were obtained at HL due to datalogger failure on Jun 29, 2015. The level sensor has a measurement range of 5 m, with an accuracy of ±0.1% FS (full scale) and a resolution of 0.03% FS. The temperature sensor has an operating range of −20 to 80°C, accuracy of ±0.1°C, and resolution of ±0.1°C. Because the water level dataloggers measure a combination of barometric pressure and water pressure, actual water pressure is obtained by calibrating the total pressure using the barometric pressure. Atmospheric pressure was measured by a self-recording barometer (Solinst® Barologger) with atmospheric pressure sensor accuracy ±0.05 kPa and temperature sensor accuracy ±0.05°C. One barometer was installed on the shore of HL and used to calibrate the water level data collected by all four water level data loggers. The lake level data is the water depth upon the level logger. For the convenience of water level comparison among lakes, the initial value of water level of each lake measured in Jun 24, 2013 was defined as zero.

Water evaporation was measured using a Class A evaporation pan installed on the water surface on the east side of HL. The water level in the evaporation pan was logged at an interval of 10 min from Jun 29, 2015 to Jul 21, 2016. Evaporation data acquisition failed between Feb 6, 2016 and Apr 5, 2016 because water was absent in the evaporation pan.

Table 1 Lake characteristics[a)]

Lake	Elevation (m)	Lake surface area (km^2)	Maximum water depth (m)	Lake water TDS ($g\ L^{-1}$)	Groundwater TDS ($g\ L^{-1}$)
BL	1208	0.11	<2	10.46*	–
NL	1179	1.44	16	105.09**	0.49**
HL	1184	1.04	10	92.31**	0.48***
YL	1153	0.96	<2	141.48*	0.71*

a) Maximum water depth, data from Yang (2002); *, data from Shao et al. (2012); **, data from Wu et al. (2014); ***, data from Gates et al. (2008a)

According to the strong correlation between evaporation and air temperature (Hu et al., 2003; Hu and Dong, 2006), the missing data were filled using ten-day mean evaporation, which was estimated from ten-day mean air temperature based on an exponential correlation (a detailed data analysis is available in Appendix A, https://link.springer.com). The freshwater from the spring at the shore of HL was used to measure evaporation. However, the studied lakes have considerable salinity difference (Table 1), and water evaporation can be affected by salinity. The daily evaporation data was calibrated using a relationship between the water surface evaporation and water salinity in BJD (Shen, 2014). The BL and YL water temperature show abnormal increasing in winter and spring, the evaporation change caused by lake water temperature was also calibrated using a relationship between the water surface evaporation and water temperature (Hu et al., 2003). Evaporation data measured by a Φ20 evaporator (an evaporation pan of diameter 20 cm) and E601B evaporation pan at Alxa Right Banner (ARB, a county) meteorological station from 2014 to 2017 were obtained from the China Meteorological Data Service Center (CMDC, http://data.cma.cn/en) for comparison. A tipping-bucket rain gauge was set up on the south side of HL in September 2014 to collect regional precipitation data. Precipitation data collected at the ARB meteorological station was also downloaded from the CMDC.

2.4 Lake water balance model

Lake water balance in the desert can be expressed by

$$\Delta S = P - E + Q_{\text{in}} - Q_{\text{out}}, \quad (1)$$

where ΔS is lake level change over unit time, P is the precipitation rate, and E is the water surface evaporation rate. Since there is no surface runoff, Q_{in} and Q_{out} represent groundwater inflow and outflow, respectively. The difference between Q_{in} and Q_{out} is defined as the groundwater net discharge rate R_G, and eq. (1) can be further transformed into

$$R_G = E - P + \Delta S. \quad (2)$$

Among the four variables in eq. (2), E, P and ΔS can be measured by evaporation pan, rain gauge and water level logger, respectively. Thus, groundwater net discharge rate R_G can be estimated using eq. (2).

3. Results

3.1 Precipitation

Precipitation data at HL and ARB is shown in Figure 2. The seasonal variation is similar at the two sites. Most rainfall events at the two stations are synchronized, especially for relatively heavy rain (>5 mm), but the total annual precipitation varies greatly. During 2015, 2016 and 2017, the total precipitation at HL was 87, 76, and 102 mm respectively, substantially lower than 141, 89, and 153 mm at ARB. Corresponding annual precipitation ratios of HL to ARB are 62%, 85% and 67% in the three years. The higher precipitation at ARB might be caused by the desert heat island effect (Wang et al., 2013). For the precipitation lower than 10 mm, there is small spatial variation in the desert. Spatial variation could be observed for the heavy rain over 10 mm, however, they still synchronously happened in the study area (Wang et al., 2013). Hence it is reasonable to use the precipitation measured at HL to represent the precipitation at other lakes.

3.2 Evaporation

The water surface evaporation at ARB measured with the Φ20 and E601B evaporation pans and evaporation at HL measured with the Class A evaporation pan are compared in Figure 3. From July 2015 to July 2016, evaporation at ARB (2063.4 mm) was much higher than that at HL (1287.7 mm).

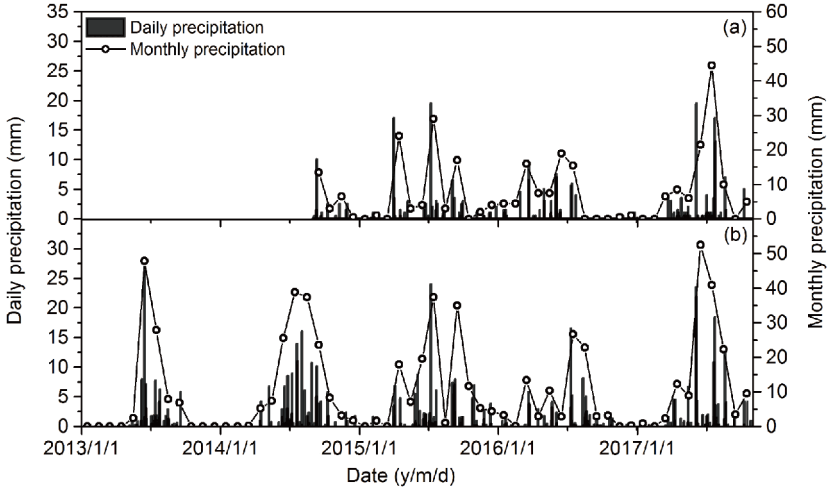

Figure 2 Daily and monthly variation of precipitation at (a) HL and (b) ARB.

Observation failures led to data gaps from August 2014 to June 2015 and August 2016 to February 2017. The missing evaporation data were filled in using the relationship between HL air temperature and Class A pan evaporation (Appendix A). The interpolated 10-day mean evaporation is shown by a blue curve in Figure 3. Direct use of the evaporation of 2600–4000 mm (Hofmann, 1999; Chen et al., 2004a, 2006; Gates et al., 2008b) measured at ARB meteorological station as the desert evaporation may overestimate the desert lake water surface evaporation.

In this study, our measured evaporation value (1287 mm) using fresh water is close to the 1100 mm that was calculated using the modified Penman equation (Yang et al., 2010). It is higher than the 935 mm measured using an E601 evaporation pan at SBL Lake (Figure 1b) from 2010 to 2011 (Dong et al., 2016). This difference may be attributed to the salinity difference (Houston, 2006; Shen, 2014). After the salinity effect calibration, the annual water evaporation at NL was estimated at 745 mm with TDS of 105 g L^{-1}. The calibrated daily evaporation values of each lake were also obtained.

3.3 Lake level variation

Figure 4 shows water level variation of all four lakes from June 2013 to February 2017. All four lake levels show similar temporal patterns, with minima in the fall, increasing from minima in fall to their maxima in the following spring, and declining through the next fall. Unlike other lakes in all years and itself in 2013–2015, YL showed additional fluctuation in January both 2016 and 2017. Its lake level first decreased to its minimum in fall as usual, but there was another minimum at the end of January. It then rapidly increased by ~0.17 m in the next 10 days.

Table 2 summarizes the level variation cycles for the four lakes. It can be seen that each lake's maximum and minimum levels were very regular, with an offset of only a few days between the years. There were time lags between the four lakes' minima and maxima every year. The level of BL reached its maximum and minimum in late March and mid-September every year, respectively, while YL in mid-April and late October. However, NL and HL synchronically reached their maxima and minima at later dates, in late April and mid-November, respectively. The four lakes also showed a substantial difference of water level variation amplitude, with a slight increasing trend from 2013 to 2016. Basically, the shallow lakes (BL and YL) showed larger amplitudes than deeper lakes (NL and HL).

3.4 Lake water temperature variation

Observed air and water temperatures of the four lakes are shown in Figure 5. All lakes' water temperatures and the air

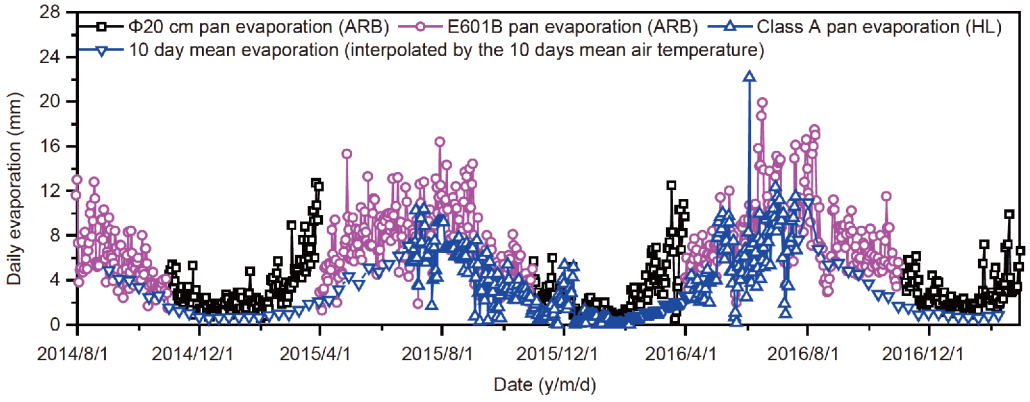

Figure 3 Daily water surface evaporation at HL and ARB.

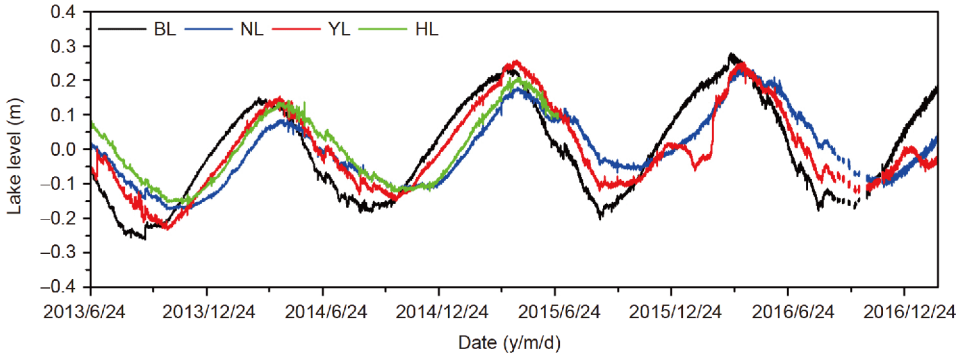

Figure 4 Lake water level variation with time.

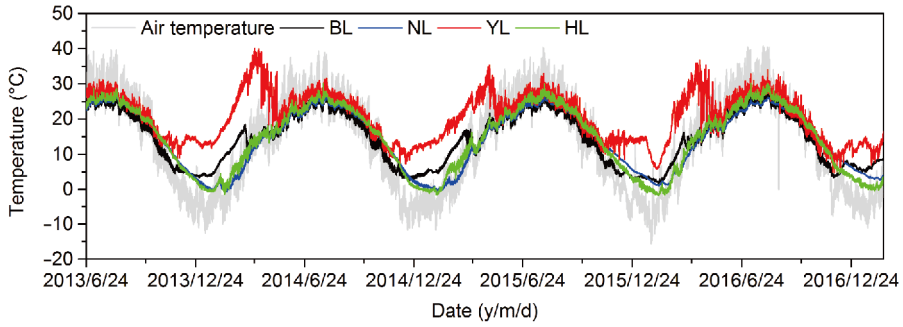

Figure 5 Lake water and air temperature variation with time.

Table 2 Lake level maximum and minimum time and variation amplitude[a)]

Lakes	2013/2014			2014/2015			2015/2016			2016/2017
	Tb	Tp	Amplitude (m)	Tb	Tp	Amplitude (m)	Tb	Tp	Amplitude (m)	Tb
BL	Sep 16, 2013	Mar 19, 2014	0.35	Sep 13, 2014	Mar 31, 2015	0.36	Sep 15, 2015	Mar 29, 2016	0.40	Sep 20, 2016
NL	Nov 11, 2013	Apr 18, 2014	0.23	Nov 21, 2014	Apr 25, 2015	0.23	Oct 30, 2015	Apr 25, 2016	0.27	Nov 16, 2016
YL	Oct 22, 2013	Apr 9, 2014	0.33	Oct 22, 2014	Apr 21, 2015	0.35	Sep 14, 2015	Apr 11, 2016	0.37	Oct 12, 2016
HL	Nov 12, 2013	Apr 20, 2014	0.27	Nov 12, 2014	Apr 27, 2015	0.30				

a) Tp and Tb represent the appearance time of lake level maximum and minimum, respectively.

temperature fluctuated similarly, suggesting that lake water temperature is mainly influenced by local air temperature. However, YL's water temperature between November and May was substantially higher than the other three lakes and the air temperature. The maxmium lake temperature at YL was 38°C in April, ~20°C higher than the air temperature in the same period. Compared to the other three lakes with minimum water temperature ~0°C in January, the minimum water temperature of YL was ~9°C in November 2013, ~8°C in December 2014, and ~6°C in February 2016. A similar abnormal water temperature increase was found at BL from November to March, but the increase was obviously less than that of YL, suggesting that heat sources besides local air temperature regulated water temperature in the BJD.

4. Discussion

4.1 Groundwater net discharge to lakes

4.1.1 Daily and annual groundwater net discharge

The groundwater net discharge rate was calculated using the lake water balance equation (eq. (2)). Lake water surface evaporation data were measured from Jun 30, 2015 to Jul 21, 2016, because the lake level measurement at HL failed from June 2015. The groundwater net discharge of lakes BL, NL and YL from Jun 30, 2015 to Jul 21, 2016 were calculated (Figure 6). It is seen that except for negative values during rainy days, groundwater net discharge values are mostly positive and have similar variations for the three lakes, indicating that they were continuously recharged by groundwater and had samilar recharge behavior.

Groundwater net discharge shows relatively large fluctuations and negative values after rainfall (Figure 6). To illustrate the detailed variation of that discharge and lake levels after precipitation, Figure 7 shows daily data of lake level, groundwater net discharge, and precipitation at three lakes during the rainy season. There was a rainfall from Jun 1 to Jun 3, 2016, with daily precipitation of 7.5, 7.0 and 1.0 mm, respectively. All three lakes' groundwater net discharge rates showed negative values during the rainy days of Jun 1 and Jun 2, 2016, then returned to positive values and increased to the maxima (i.e., ~18 mm d^{-1} at BL, 15 mm d^{-1} at NL and 13 mm d^{-1} at YL) on Jun 3. This regularity was also found in other rainfall events. On rainy days, the lake level can immediately increase as precipitation falls directly on the lake surface. However, the phreatic water table cannot increase so rapidly because it takes time for surface water to infiltrate the soil to reach the groundwater table. Therefore, the lake level should exert a higher pressure on the surrounding phreatic water level after rainfall, causing lake water recharges to the phreatic aquifer (i.e., negative groundwater net discharge values). With the precipitated water infiltrating to the phreatic water table after rainfall (normally 1–2 days), the phreatic water level rises, and the groundwater net discharge increases to positive and rapidly reaches its maximum. Local precipitation can recharge the phreatic water and then recharge the lakes via the groundwater. An obvious groundwater net discharge peak appeared after a rainfall higher than 7 mm d^{-1} (Figure 6). This indicates that only heavy rainfalls can infiltrate and recharge

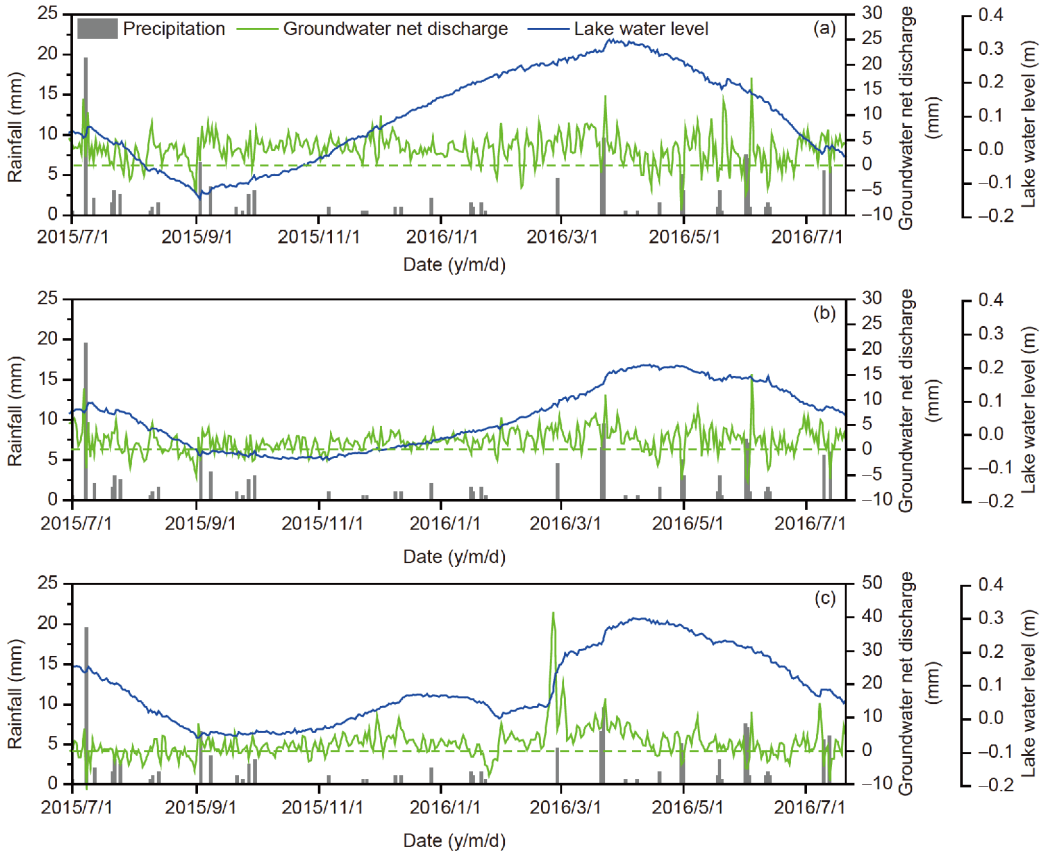

Figure 6 Precipitation, lake level and groundwater net discharge variation with time. (a) BL; (b) NL; (c) YL.

the phreatic water and lakes.

To investigate seasonal variations of groundwater net discharge, monthly average discharges were obtained from multiyear observation records, BL, NL and YL from Sep 1, 2014 to Feb 15, 2017, and HL from only Sep 1, 2014 to Jun 28, 2015 because of instrument failure. Excepting the period Jun 30, 2015 to Jul 21, 2016 with measured evaporation, evaporation in other periods was estimated using the correlation with air temperature (Figure 3 and Appendix A). Figure 8 shows the monthly mean rainfall, evaporation, lake level and estimated groundwater net discharge of all four lakes. Lake level seasonal variation in BJD is mainly controlled by water surface evaporation and groundwater discharge. Lake levels increase during the period around October through April with groundwater net discharge exceeding evaporation (yellow shading in Figure 8). From April through September, groundwater net discharge is less than evaporation, and the lakes level decreases. In contrast, groundwater net discharge reaches high values during October to April and stays low during the raining season (e.g. May to September).

From Jul 1, 2015 to Jun 30, 2016, the average groundwater net discharge rate of BL, NL and YL was estimated at 3.06, 1.79 and 2.39 mm d^{-1}, respectively, leading to annual discharge amounts of 1121.7, 655.3 and 875.3 mm. These values are different from groundwater discharge values of 898–1024.6 mm obtained at SBL (Figure 1b) (Dong et al., 2016; Gong et al., 2016). From short-term summer isotope data, the average groundwater net discharge rate at SL (Figure 1b) is ~6 mm d^{-1} (Luo et al., 2016, 2017). These results suggest that lakes have different groundwater net discharge in BJD. The groundwater net discharge does not depend on the lake area, depth, and their evaporation, the biggest lake NL has the lowest groundwater net discharge (Figure 8). Among the three studied lakes, the highest groundwater net discharge of 1121.7 mm (BL) is about 1.7 times of the lowest 655.3 mm (NL). These results suggest that the hydrogeology characteristics of the aquitards underlying the studied lakes control the groundwater net discharge rate.

4.1.2 Hourly groundwater net discharge

Six non-rainy days between May 25 and May 30, 2016 were selected to analyze the hourly variation of lake level, lake level change (the lake level difference between hour t+1 and t), evaporation, and groundwater net discharge. The hourly data were averaged over six days (Figure 9) to examine their diurnal variation patterns. All three lakes show similar lake level fluctuations, with a semidiurnal cycle. All lake levels increased from about 7:00, reaching relatively high peak

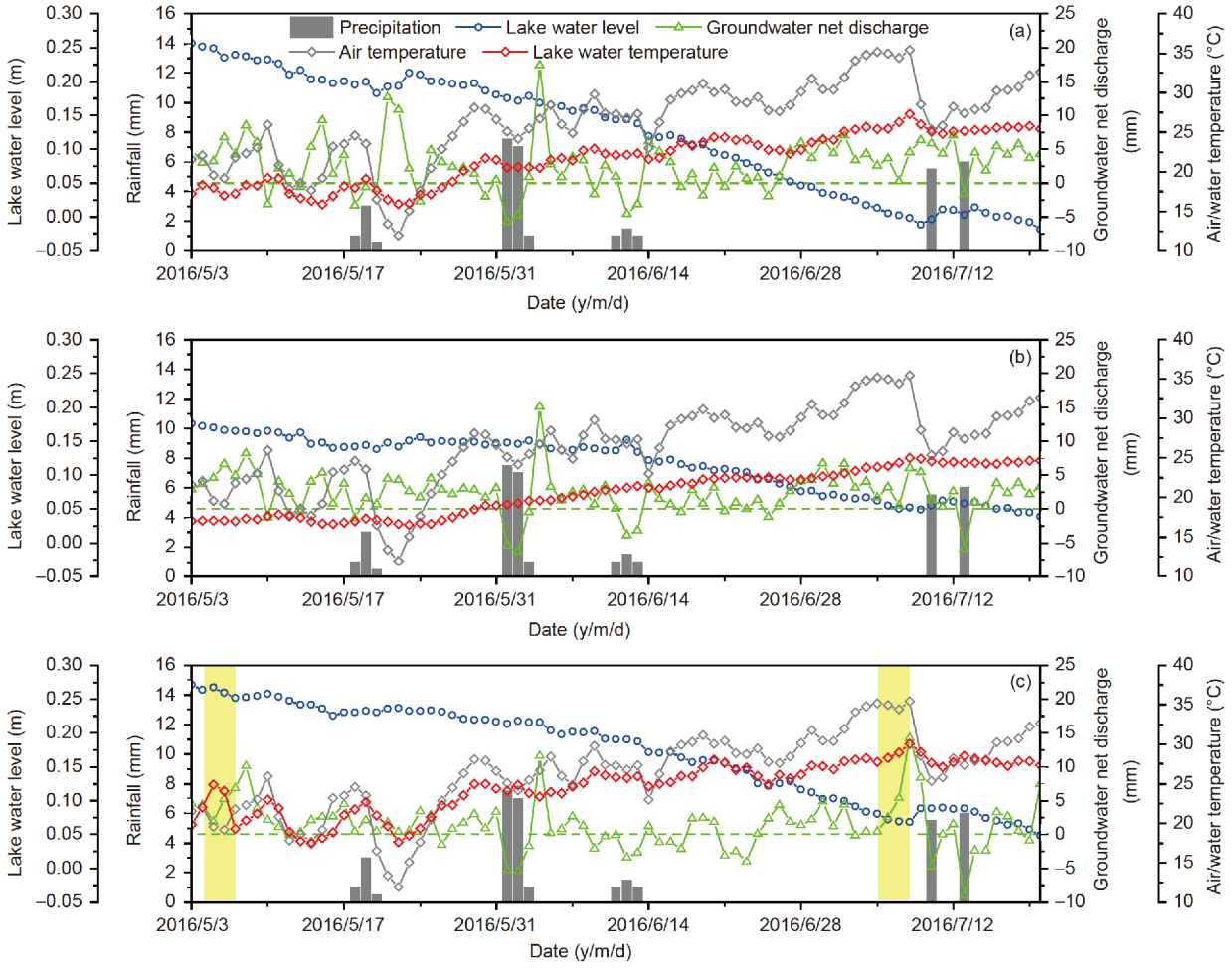

Figure 7 Daily lake water level, groundwater net discharge rate, rainfall, air temperature and lake water temperature variation with time. (a) BL; (b) NL; (c) YL.

values at 14:00, and then decreased until 21:00. They increased again and reached a relatively small peak at 2:00 the subsequent morning, and then decreased until 7:00. The lake surface evaporation had a 24-hour cycle (Figure 9) crossing daytime and nighttime. It is interesting that lake level fluctuation could reach about five times as that of evaporation. Hence, evaporation could not generate that large lake level fluctuation. Because there was no rainfall in the period, the hourly lake level variations were mainly altered by groundwater net discharge. The groundwater net discharge showed patterns similar to lake's water level change, with positive values from 7:00 through 14:00 and 21:00 through 2:00. The hourly lake level variation and groundwater net discharge over 24 hours cannot be explained by the evaporation, so there must involve other mechanisms. Richter et al. (2015) showed that the maximum amplitude of the lake tide can only reach about 3 mm, even in large lakes (e.g., Lago Argentino, South America) covering thousands of square kilometers. However, the studied lakes' diurnal amplitude reached ~10 mm. The diurnal amplitude might be caused by earth tide and atmospheric pressure. Under these two forces, diurnal water level variation in wells and bores were widely reported (Kopylova et al., 2009; Acworth and Brain, 2008; Yang and Wei, 2018; Zhang et al., 2008).

Positive values of groundwater net discharge represent a net inflow water amount to the lakes, and negative values indicate net outflow. BL, NL and YL had average net inflow and outflow values of 11.59 and 9.24, 12.37 and 9.09, and 10.87 and 9.61 mm d^{-1} during the six days in May, respectively. The difference between inflow and outflow should be consumed by evaporation and thereby caused the lake level variation. Such differences can reach 2.35, 3.28 and 1.26 mm d^{-1} for the three lakes respectively. Comparing to the mean evaporation of 5.09, 3.65 and 4.05 mm d^{-1}, these difference values indicate that the lake level decreased during the six days (Figure 9).

The inflow-outflow analysis reveals that all three lakes are groundwater flow-through lakes. The desert lakes usually represent outcrops of regional groundwater (Jiao et al., 2015; Yechieli and Wood, 2002; Luo et al., 2017). As shown in Figure 1b, lake levels in the southeast were higher than those in the northwest, with a groundwater flow direction from

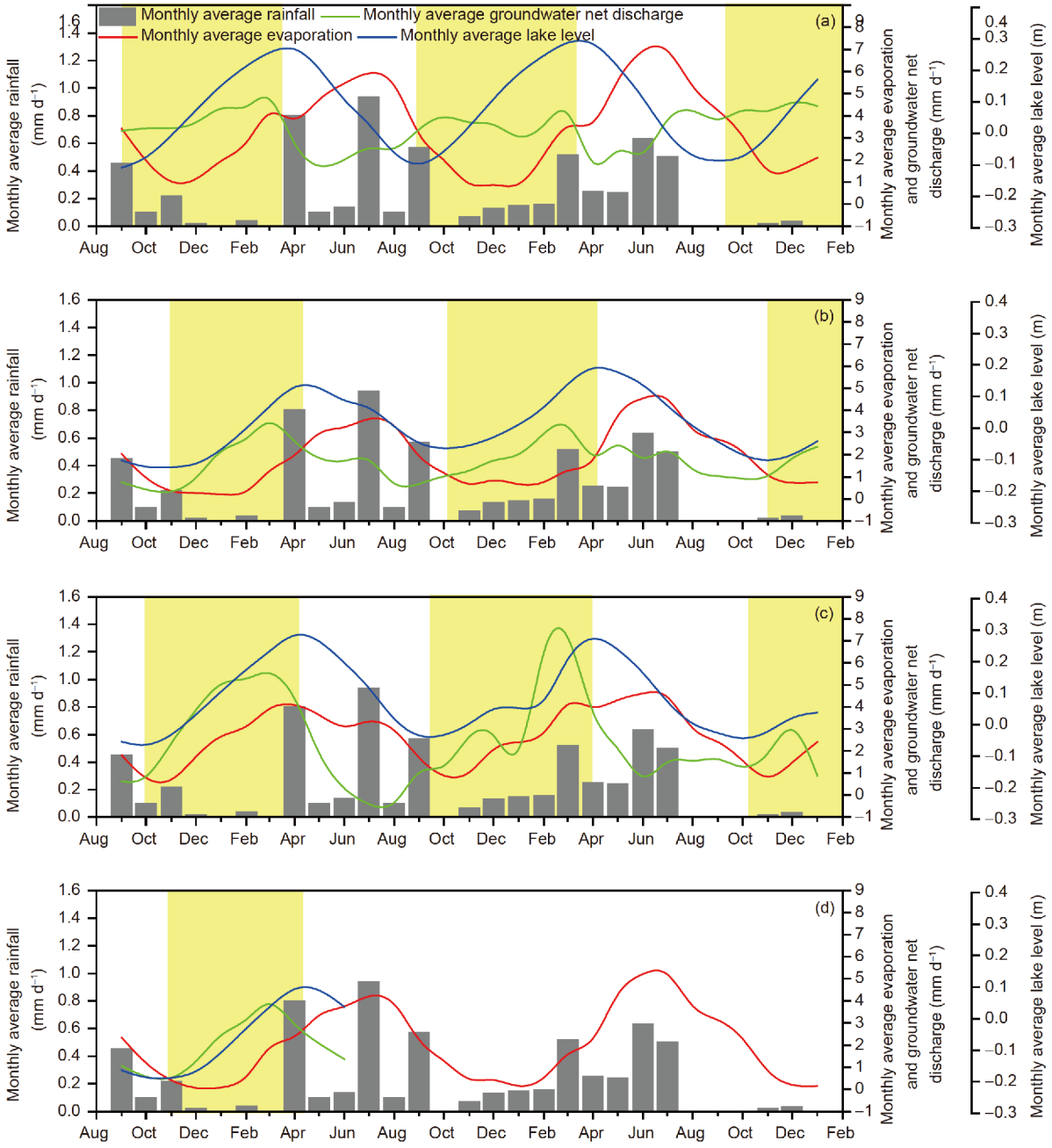

Figure 8 Monthly mean precipitation, evaporation, lake level and groundwater net discharge variation of four studied lakes. (a) BL; (b) NL; (c) YL and (d) HL.

southeast to northwest. The groundwater ion concentration slowly increased along this direction (Shao et al., 2012), and the lake water shows a trend of sub-saline to saline and hyper-saline from the southeast to northwest (Shao et al., 2012; Chen et al., 2012; Dong et al., 2016; Yang and Williams, 2003). This salinity gradient may be attributable to outflow salinity accumulation along the groundwater flow direction. The outflow also explains there is a brackish pore water zone around the brine lakes (Luo et al., 2016, 2017). However, most groundwater in the desert is fresh water and provides drinking water to local herdsman. This indicates that the salinity loss from lakes via the outflow is limited, although there is outflow from the lakes.

4.2 Origin of groundwater in the desert

The temporal patterns of groundwater discharge rate are informative to the origin of the groundwater in the BJD. The groundwater discharge rate to lakes increased after rainfall events (Figure 7), and monthly groundwater discharge rates

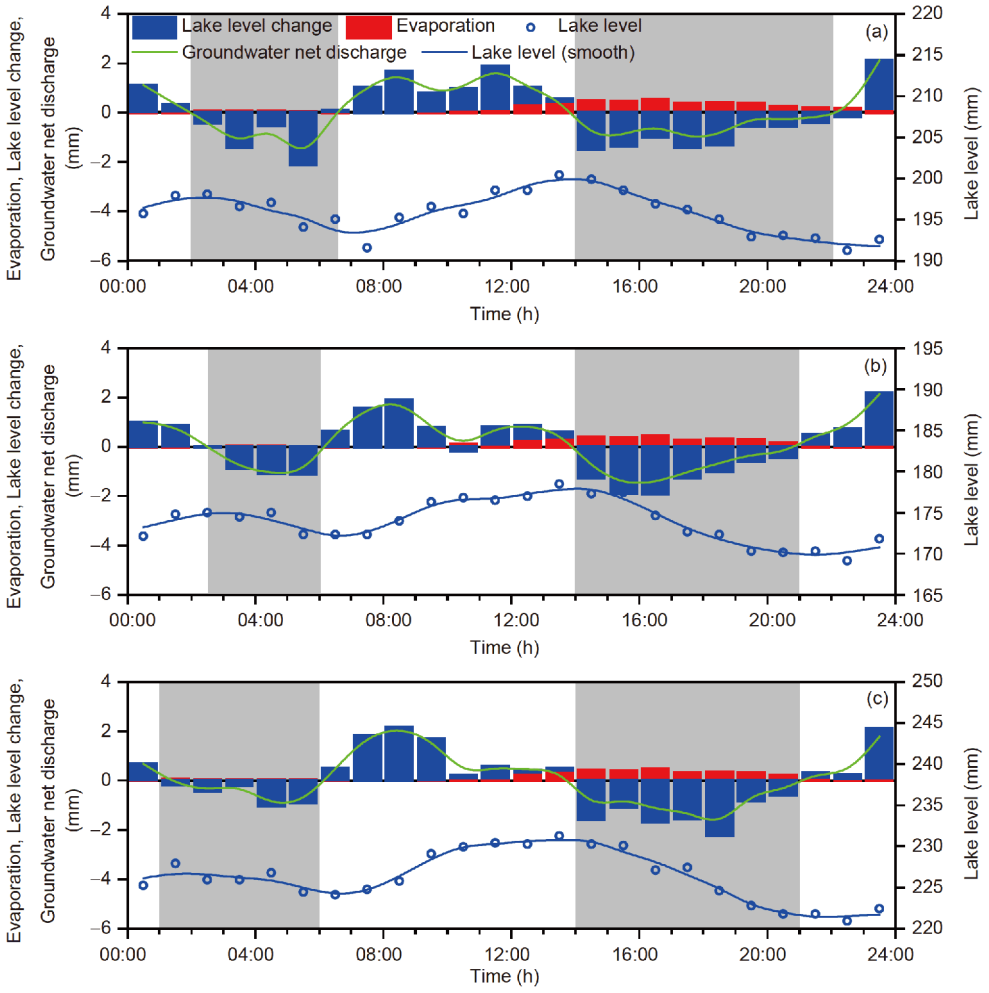

Figure 9 Hourly variation of lake level and groundwater net discharge; data are six-day averages. Lake level was smoothed using Savitzky-Golay method with second-order polynomial and 3-point moving window. (a) BL; (b) NL; (c) YL.

were slightly increased during rainy months (Figure 8). All this evidence suggests that local precipitation is one of the recharge sources of the phreatic water.

In winter and spring, YL and BL water temperatures were abnormally higher than air temperature (Figure 5). As the air temperature decreased, the lake water temperature increased abnormally (Figure 5; yellow shading in Figure 7). The only explanation is that the two lakes were recharged seasonally by deep aquifer water with high temperature. This deep groundwater is at least 20°C warmer than the lake water (Figure 5). Given an average geothermal gradient in this area of approximately 2.51–3.00°C/100 m (Ren et al., 2000), the deep groundwater is coming from more than 600 m below the ground surface.

In summer and autumn, owing to the high air and water temperatures, abnormal variation of lake water temperature is too subtle to observe. From Jun 27 to Jul 6, 2016, BL, NL and YL showed a relatively large groundwater net discharge. In particular for YL, there was an obvious groundwater net discharge peak on Jul 6, 2016 (Figure 7). Because there were no precipitation events in the desert and at ARB during this period, this groundwater net discharge peak might have been caused by the increase of warm confined water. There were also several abnormal water temperature increases when air temperature dropped (yellow shading in Figure 7). Hence, we conclude that in summer and autumn, the thermal deep groundwater intermittently recharged the lakes. For NL and HL, there were only slight water temperature abnormalities in March (Figure 5), likely due to their high water volume as they are big and deep (Table 1). The warm confined groundwater only had a limited influence on the water temperature of large lakes. The same abnormally high water temperature was also found in other lakes (SL, ZL and NGL; Figure 1b) (Dong et al., 2016). Therefore, we conclude that the desert lakes are recharged by the thermal confined groundwater. The high water temperature in winter and spring, and its intermittent occurrence in summer and autumn indicate that the deep confined warm groundwater may recharge seasonally and that its amount in summer and autumn is very limited. The pool of this deep groundwater

source likely originated from Qilian Mountains or Qinghai-Tibetan Plateau (Chen et al., 2003, 2004a, 2004b; Zhao and Chen, 2006) but need further evidences.

4.3 Trend of lake level change

The level of the four lakes showed an inter-annual trend from 2013 to 2017 (Figure 4). We used the EMD method (Appendix B) to analyze trends of monthly rainfall and lake level variation. Rainfall and lake levels of BL, NL, and HL show an increasing trend over the recent four years. The lake levels of NL and BL increased about 7 and 10 cm from June 2013 to February 2017, respectively. The water levels of BL, NL and HL increased in the past four years, but at relatively low rates, 1.85, 1.80 and 2.4 cm yr^{-1}, respectively (Figure 10). This indicates that under the present natural condition, the lake water can maintain an approximate balance and the lake water recharge seems a little bit higher than the discharge.

The lake level of YL initially increased through early 2016 and then decreased, and the decreasing rate reached 12.10 cm yr^{-1} (Figure 10), much greater than the increasing rate of the other three lakes. Desert lake water level was mainly controlled by water surface evaporation and groundwater discharge. The evaporation increase caused by the abnormal lake water temperature increase might led to the decrease of lake level for YL, however, abnormal water temperature increase can also be found in other period, i.e. spring of 2014 to 2016 (Figure 5), the increase extent of abnormal lake water temperature at YL in 2014 even higher than that in 2015 and 2016, but the lake level are still increased at YL from 2014 to 2015. This indicated that the YL lake level decrease should be affected by other factors. The YL lake level decrease from the beginning of 2016 was likely attributable to a decline in groundwater recharge. The abnormal decrease of YL level was caused by surrounding groundwater recharge variation. However, the reason of groundwater recharge variation is unclear and need further study.

5. Conclusions

This paper estimates groundwater net discharge rate for four representative lakes in BJD using four-year water level data together with precipitation and evaporation, analyzes their temporal patterns, and discusses groundwater sources. The following conclusions can be drawn.

(1) The lake level seasonal fluctuation is mainly regulated by water surface evaporation and groundwater discharge. From October through April, the groundwater discharge rate is greater than evaporation, raising lake levels. Lake levels decline in the other half-year as a result of lake water surface evaporation exceeding the groundwater discharge.

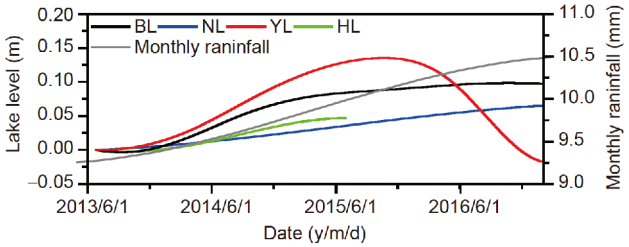

Figure 10 Secular trend of lake level and rainfall.

(2) Phreatic water and lakes in the BJD are also recharged by deep confined warm groundwater in addition to precipitation, but this groundwater is only intermittent, with a high discharge rate in winter and spring.

(3) The lakes not only have groundwater inflow and recharge but also outflow to groundwater. The lakes are connected by groundwater and have similar recharge and discharge pattern in the BJD, but show different net discharge rates of three studied lakes of 1.79 mm d^{-1} for NL, 2.39 mm d^{-1} for YL and 3.06 mm d^{-1} for BL, respectively.

(4) The EMD method is used to identify lake level trends. In a recent four years, the overall lake levels increased with the local precipitation. However, individual lake level decreased after 2016, which may be caused by its surrounding groundwater recharge variation.

Acknowledgements *We thank the three reviewers for their helpful suggestions and comments. The work was supported by the Strategic Priority Research Program of Chinese Academy of Sciences, Pan-Third Pole Environment Study for a Green Silk Road (Pan-TPE) (Grand No. XDA20090000), the National Natural Science Foundation of China (Grand No. 41771016) and NASA's Surface Water and Ocean Topography (SWOT) Program (Grand No. NNX16A85G).*

References

Acworth R I, Brain T. 2008. Calculation of barometric efficiency in shallow piezometers using water levels, atmospheric and earth tide data. Hydrogeol J, 16: 1469–1481

Chen L, Wang N A, Wang H, Dong C Y, Lu Y, Lu J W. 2012. Spatial patterns of chemical parameters of lakes and groundwater in Badain Jaran Desert (in Chinese with English abstract). J Desert Res, 32: 531–538

Chen J S, Fan Z, Wang J, Gu W, Zhao X. 2003. Isotope methods for studying the replenishment of the lakes and downstream groundwater in the Badain Jaran Desert (in Chinese with English abstract). Acta Geosci Sin, 24: 497–504

Chen J S, Li L, Wang J Y, Barry D A, Sheng X F, Gu W Z, Zhao X, Chen L. 2004a. Groundwater maintains dune landscape. Nature, 432: 459–460

Chen J, Zhao X, Wang J, Gu W, Sheng X, Su Z. 2004b. Meaning of the discovery of lacustrine tufa and root-shaped nodule in Badain Jaran Desert for the study of lake recharge (in Chinese with English abstract). Carsol Sin, 23: 277–282

Chen J S, Zhao X, Sheng X F, Dong H Z, Rao W B, Su Z G. 2006. Formation mechanisms of megadunes and lakes in the Badain Jaran Desert, Inner Mongolia. Chin Sci Bull, 51: 3026–3034

Dong C, Wang N, Chen J, Li Z, Chen H, Chen L, Ma N. 2016. New observational and experimental evidence for the recharge mechanism of

the lake group in the Alxa desert, North-central China. J Arid Environ, 124: 48–61
Dong Z, Qian G, Lv P, Hu G. 2013. Investigation of the sand sea with the tallest dunes on Earth: China's Badain Jaran Sand Sea. Earth-Sci Rev, 120: 20–39
Gao Q, Tao Z, Li B, Jin H, Zou X, Zhang Y, Dong G. 2006. Palaeomonsoon variability in the southern fringe of the Badain Jaran Desert, China, since 130 ka BP. Earth Surf Process Landf, 31: 265–283
Gates J B, Edmunds W M, Darling W G, Ma J, Pang Z, Young A A. 2008a. Conceptual model of recharge to southeastern Badain Jaran Desert groundwater and lakes from environmental tracers. Appl Geochem, 23: 3519–3534
Gates J B, Edmunds W M, Ma J, Scanlon B R. 2008b. Estimating groundwater recharge in a cold desert environment in northern China using chloride. Hydrogeol J, 16: 893–910
Gong Y P, Wang X S, Hu B X, Zhou Y X, Hao C B, Wan L. 2016. Groundwater contributions in water-salt balances of the lakes in the Badain Jaran Desert, China. J Arid Land, 8: 694–706
Hofmann J. 1999. Geoökologische untersuchungen der gewässer im südosten der Badain Jaran Wüste (Aut. Region Innere Mongolei/VR China)-status und spätquartäre gewässerentwicklung. Berliner Geographische Abhandlungen, 64: 1–247
Hou L Z, Wang X S, Hu B X, Shang J, Wan L. 2016. Experimental and numerical investigations of soil water balance at the hinterland of the Badain Jaran Desert for groundwater recharge estimation. J Hydrol, 540: 386–396
Hu A Y, Dong X G. 2006. A study on water surface evaporation in southern Xinjiang (in Chinese with English abstract). J Arid Land Resour Environ, 20: 22–24
Hu S J, Wang J L, Song Y D, Zhang Q, Li Y H, Chen X B. 2003. An experimental research on the water surface evaporation in Tarim River Basin (in Chinese with English abstract). J Arid Land Resour Environ, 17: 95–98
Huang T M, Pang Z H. 2007. Groundwater recharge in Badain Jaran Desert and Gurinai Oasis based on environmental tracers (in Chinese with English abstract). Geoscience, 21: 624–631
Houston J. 2006. Evaporation in the Atacama Desert: An empirical study of spatio-temporal variations and their causes. J Hydrol, 330: 402–412
Jiao J J, Zhang X, Wang X. 2015. Satellite-based estimates of groundwater depletion in the Badain Jaran Desert, China. Sci Rep, 5: 8960
Kopylova G N, Gorbunova E M, Boldina S V, Pavlov D V. 2009. Estimation of deformational properties of a stratum-borehole system based on analysis of barometric and tidal responses of the water level in a borehole. Izv Phys Solid Earth, 45: 905–913
Luo X, Jiao J J, Wang X, Liu K. 2016. Temporal ^{222}Rn distributions to reveal groundwater discharge into desert lakes: Implication of water balance in the Badain Jaran Desert, China. J Hydrol, 534: 87–103
Luo X, Jiao J J, Wang X, Liu K, Lian E, Yang S. 2017. Groundwater discharge and hydrologic partition of the lakes in desert environment: Insights from stable ^{18}O/^{2}H and radium isotopes. J Hydrol, 546: 189–203
Ma J Z, Edmunds W M. 2006. Groundwater and lake evolution in the Badain Jaran Desert ecosystem, Inner Mongolia. Hydrogeol J, 14: 1231–1243
Ma J Z, Huang T M, Ding Z Y, Edmunds W M. 2007. Environmental isotopes as the indicators of the groundwater recharge in the south Badain Jaran Desert (in Chinese with English abstract). Adv Earth Sci, 22: 922–930
Ma Y D, Zhao J B, Luo X Q, Shao T J, Dong Z B, Zhou Q. 2017. Hydrological cycle and water balance estimates for the megadune-lake region of the Badain Jaran Desert, China. Hydrol Process, 31: 3255–3268
Ren Z L, Liu C Y, Zhang X H, Wu H N, Chen G, Li J B, Ma T X. 2000. Recovery and comparative research of thermal history on Jinquan Basin Group. Chin J Geophys, 43: 635–645
Richter A, Marderwald E, Hormaechea J L, Mendoza L, Perdomo R, Connon G, Scheinert M, Horwath M, Dietrich R. 2015. Lake-level variations and tides in Lago Argentino, Patagonia: Insights from pressure tide gauge records. J Limnol, 75: 62–77
Shao T J, Zhao J B, Zhou Q, Dong Z B, Ma Y D. 2012. Recharge sources and chemical composition types of groundwater and lake in the Badain Jaran Desert, northwestern China. J Geogr Sci, 22: 479–496
Shen S P. 2014. Based on the observation of the Badain Jaran Desert lake evaporation salinity effect research (in Chinese with English abstract). Dissertation for Master Degree. Lanzhou: Lanzhou University
Wang N A, Ma N, Chen H B, Chen X L, Dong C Y, Zhang Z Y. 2015. Formation and evolution of the Badain Jaran Desert, North China, as revealed by a drill core from the desert centre and by geological survey. Palaeogeogr Palaeoclimatol Palaeoecol, 426: 139–158
Wang N A, Ma N, Chen H B, Chen X L, Dong C Y, Zhang Z Y. 2013. A preliminary study of precipitation characteristics in the hinterland of Badian Jaran Desert (in Chinese with English abstract). Adv Water Sci, 24: 153–160
Wang X S, Hu B X, Jin X M, Hou L Z, Qian R Y, Wang L D. 2014. Interactions between groundwater and lakes in Badain Jaran Desert (in Chinese with English abstract). Earth Sci Front, 21: 91–99
Wu X, Wang, X S, Wang Y, Hu B X. 2017. Water resources in the Badain Jaran Desert, China: New insight from isotopes. Hydrol Earth Syst Sci, 21: 4419–4431
Wu Y, Wang N A, Zhao L Q, Zhang Z Y, Chen L, Lu Y, Lü X N, Chang J L. 2014. Hydrochemical characteristics and recharge sources of Lake Nuoertu in the Badain Jaran Desert. Chin Sci Bull, 59: 886–895
Wu Z, Huang N E, Long S R, Peng C K. 2007. On the trend, detrending, and variability of nonlinear and nonstationary time series. Proc Natl Acad Sci USA, 104: 14889–14894
Wu Z, Huang N E, Wallace J M, Smoliak B V, Chen X. 2011. On the time-varying trend in global-mean surface temperature. Clim Dyn, 37: 759–773
Yan M, Wang G, Li B, Dong G. 2001. Pleistocene paleowind direction change in the Badain Jaran Desert and its environmental significance (in Chinese with English abstract). J Tsinghua Univ-Sci Technol, 41: 118–122
Yang X L, Wei Z G. 2018. Response characteristics of water level to atmospheric loading and solid earth tide in different frequency bands: A case study of the Shiquan well, Shanxi (in Chinese with English abstract). Geodesy Geodyn, 38: 1096–1100
Yang X P. 2002. Water chemistry of the lakes in the Badain Jaran Desert and their Holocene evolutions (in Chinese with English abstract). Quat Sci, 22: 97–104
Yang X P, Williams M A J. 2003. The ion chemistry of lakes and late Holocene desiccation in the Badain Jaran Desert, Inner Mongolia, China. Catena, 51: 45–60
Yang X P, Liu T S, Xiao H L. 2003. Evolution of megadunes and lakes in the Badain Jaran Desert, Inner Mongolia, China during the last 31000 years. Quat Int, 104: 99–112
Yang X P, Ma N N, Dong J F, Zhu B Q, Xu B, Ma Z B, Liu J Q. 2010. Recharge to the Inter-Dune Lakes and Holocene climatic changes in the Badain Jaran Desert, Western China. Quat Res, 73: 10–19
Yang X, Scuderi L, Liu T, Paillou P, Li H, Dong J, Zhu B, Jiang W, Jochems A, Weissmann G. 2011. Formation of the highest sand dunes on Earth. Geomorphology, 135: 108–116
Yechieli Y, Wood W W. 2002. Hydrogeologic processes in saline systems: Playas, sabkhas, and saline lakes. Earth-Sci Rev, 58: 343–365
Zhang J. 2015. Studies on key hydrogeological problems in the Western Alxa, China (in Chinese with English abstract). Doctoral Dissertation. Beijing: China University of Geosciences
Zhang J, Wang X S, Hu X N, Lu H P, Gong Y P, Wan L. 2015. The macro-characteristics of groundwater flow in the Badain Jaran Desert (in Chinese with English abstract). J Desert Res, 35: 774–782
Zhang J, Wang X S, Hu X N, Lu H T, Ma Z. 2017. Research on the recharge of the lakes in the Badain Jaran Desert: Simulation study in the Sumu Jaran lakes area. J Lake Sci, 29: 467–479
Zhang W H, Mei J C, Li J M, Li J G. 2008. Study on water-well earth tide and atmospheric response in three gorger well network (in Chinese with

English abstract). J Geodesy Geodyn, 28: 45–49
Zhang Z Y, Wang N A, Ma N, Dong C Y, Chen L, Shen S P. 2012. Lakes area change in Badain Jaran Desert hinterland and its influence factors during the recent 40 years (in Chinese with English abstract). J Desert Res, 32: 1743–1750
Zhang Z Y, Wang N A, Wu Y, Shen S P, Zhang X H, Chang J L. 2013. Remote sensing on spatial changes of lake area in Badain Jaran Desert hinterland during 1973–2010. J Lake Sci, 25: 514–520
Zhao X, Chen J S. 2006. Application of similarity priority ratio on resources of groundwater in Badain Jaran Desert and its surrounding areas. J Lake Sci, 18: 407–413
Zhao J B, Ma Y D, Luo X Q, Yue D P, Shao T J, Dong Z B. 2017. The discovery of surface runoff in the megadunes of Badain Jaran Desert, China, and its significance. Sci China Earth Sci, 60: 707–719
Zhu J F, Wang N A, Li Z L, Dong C Y, Lu Y, Ma N. 2011. RS-based monitoring seasonal changes of lake in Badain Jaran Desert (in Chinese with English abstract). Lake Sci, 23: 657–664
Zhu Z D, Wu Z, Liu S, Di X M. 1980. Deserts in China (in Chinese). Beijing: Science Press. 107

(Responsible editor: Jianhui CHEN)